# Characterization and Comparison of Landsat-4 and Landsat-5 Thematic Mapper Data*

*Michael D. Metzler* and *William A. Malila*
Environmental Research Institute of Michigan, P.O. Box 8618,
Ann Arbor, MI 48107

ABSTRACT: Analyses of the characteristics of Landsat Thematic Mapper (TM) image data are described, and results are summarized. Emphasis is placed on radiometric characterization, development of response models, and on comparisons between data from Landsats 4 and 5. In general, the data quality was excellent; however, some anomalies were found. Three main topics are (a) systematic within-scan-line signal droop/rise, (b) random scan-correlated level shifts, and (c) radiometric (signal amplitude) relationships between Landsat-4 and Landsat-5. The systematic droop/rise effect was found in data from both Landsats 4 and 5. Daytime signals droop across the scan line while nighttime signals in the reflective bands rise across the scan line. The magnitude of the droop/rise appears to be a function of the signal magnitude and average value of the signal throughout a scan cycle. Scan-correlated level-shift noise also was observed in data from both sensors, but with different patterns. Low-amplitude, low-frequency coherent noise effects also were measured. The analysis of simultaneously acquired Landsat-4 and Landsat-5 TM data permitted a direct empirical comparison of the relative radiometric responses of their respective spectral bands. Relationships between their respective signal values were developed, and sensor dynamic range considerations are discussed. It was determined that multiplicative factors ranging from 0.987 to 1.145 were required to convert the signal counts from Landsat-4 TM spectral bands to corresponding Landsat-5 equivalent signals. Radiance values exhibited corresponding differences, pointing to residual errors in radiometric calibration. Low-level clipping was evident in the radiometrically corrected Landsat-5 bands 5 and 7 data. The temperature range covered by the full 8-bit data range of TIPS-processed TM band 6 data was found to be approximately 200°K to 340°K, not 260°K to 320°K as specified.

## INTRODUCTION

SINCE THE LAUNCH of Landsat-4 in July 1982, numerous studies of the quality of Thematic Mapper (TM) image data have been performed under the auspices of the National Aeronautics and Space Administration's (NASA's) Landsat Image Data Quality Analysis (LIDQA) Program. As part of this program, we have performed engineering analyses of Thematic Mapper image data with our efforts concentrated on radiometric characterization of the sensor. In general, we have found the data quality to be excellent. However, anomalies do exist in the data from both Landsat-4 and Landsat-5 TM. The analyses of Landsat-4 TM image data were previously described in detail by the authors (Metzler and Malila, 1983b; Malila *et al.*, 1984; Metzler and Malila, 1983a) and are summarized below. This paper concentrates on recent analyses of Landsat-5 TM data and comparisons of the radiometry of the two sensors. Specific topics covered are (a) within-line droop, a phenomenon whereby the signal levels of the sensor change systematically during the active scan; (b) scan-correlated level shifts, an effect which raises or lowers the signal level of all pixels in a scan line or set of scan lines; and (c) comparison of Landsat-4 and Landsat-5 radiometric corrections. Other analyses of TM data anomalies may be found elsewhere in this issue (e.g., Kieffer *et al.*, 1985).

### WITHIN-LINE DROOP

Earlier examination of Landsat-4 TM average scan lines indicated significant differences in the signals returned from the western edge of a scene compared to those observed at the eastern edge of the same scene. This effect was most apparent in the shortest wavelength spectral band (band 1), and was observed in all the spectral bands to some extent. A combination of bidirectional reflectance, atmospheric, and shadowing effects, as well as sun-view angle geometry can explain the effect observed. More careful examination of the average scan data, however, revealed a confounding effect due to dif-

* This research was sponsored by the U.S. National Aeronautics and Space Administration, Goddard Space Flight Center, Greenbelt, MD, under Contract NAS5-27346.

PHOTOGRAMMETRIC ENGINEERING AND REMOTE SENSING,
Vol. 51, No. 9, September 1985, pp. 1315-1330.

0099-1112/85/5109-1315$02.25/0

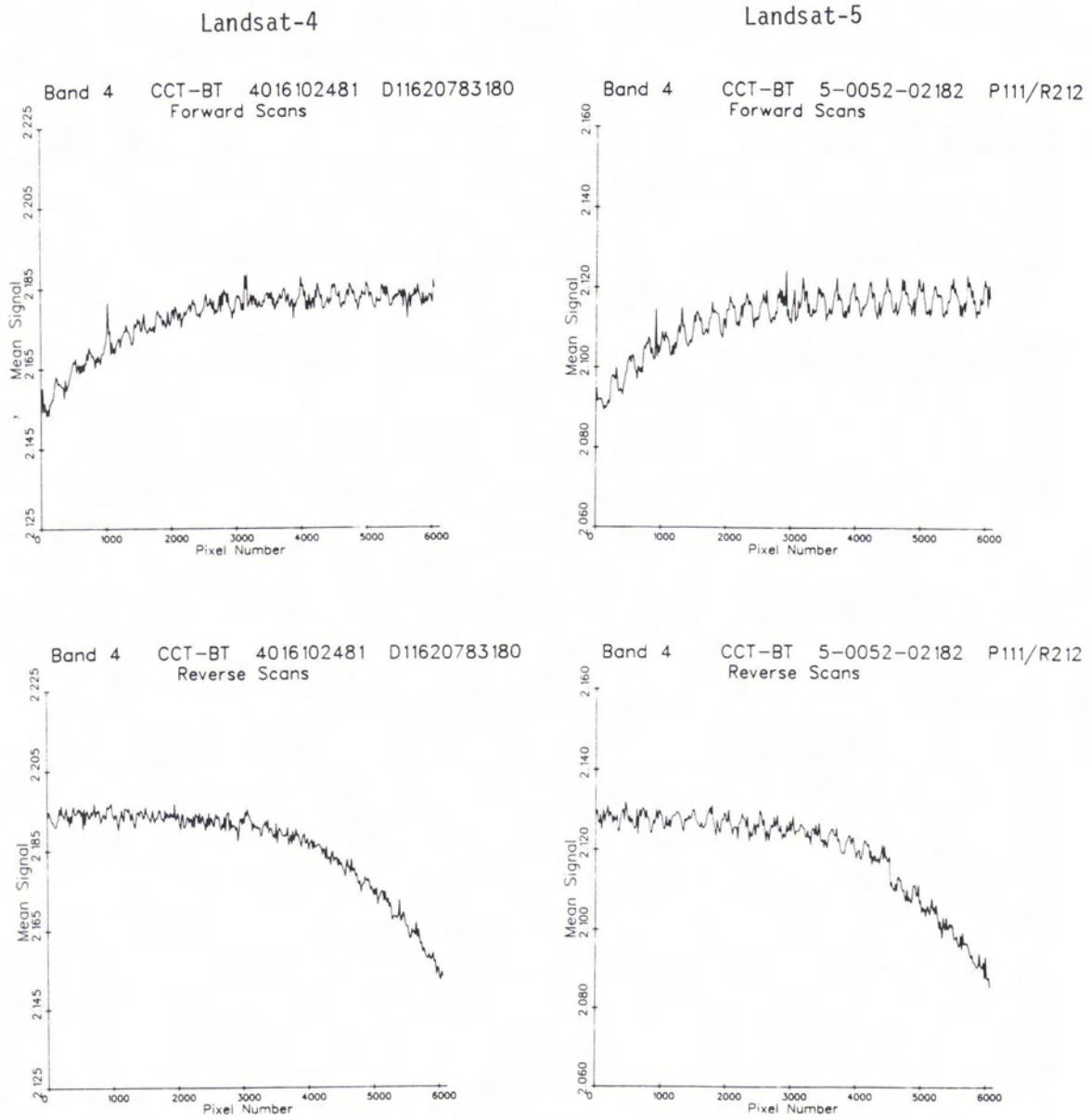


FIG. 1. Landsat-4 and Landsat-5 TM nighttime within-scan rise effect—band 1.

ferent sensor response characteristics related to the direction of scan in bands 1 through 4. The scan-direction difference took the form of a droop in signal with time during active scan, which appeared as a signal decrease with increasing pixel number for forward scans, and a signal increase with increasing pixel number for reverse scans. This effect was found in nighttime reflective-band data as well, but taking the form of a signal rise with time instead of a droop.

## SCAN-CORRELATED LEVEL SHIFTS

In Landsat-4 TM data, an effect was analyzed which changed the signal of all samples within a scan-line or group of scan-lines by up to 2.0 video quantum levels (DN). The changes were aperiodic, occurring at random intervals with the level shifting during mirror turn-around time. All affected detectors shifted levels at the same time, with the level shifts following one of two patterns (most detectors

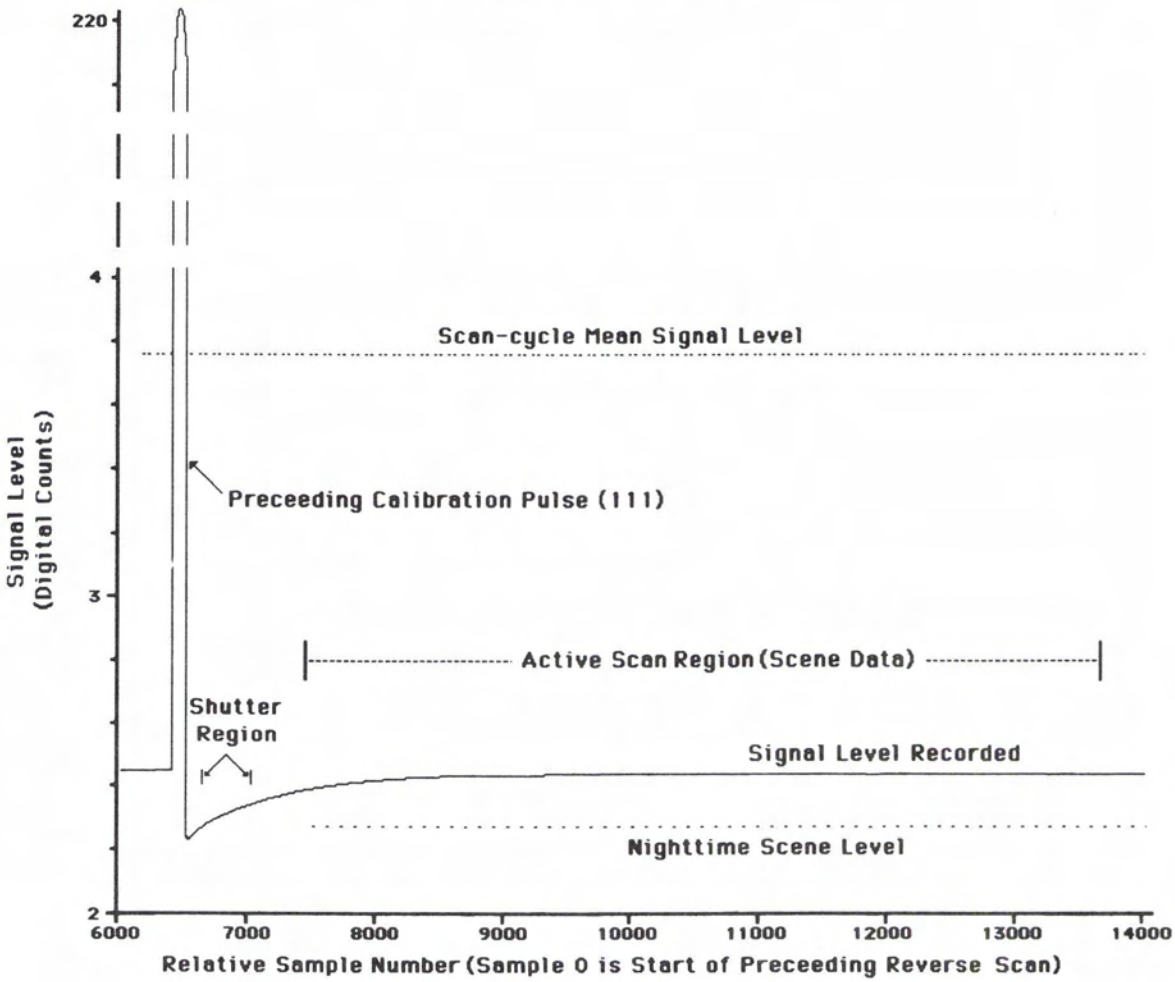


FIG. 2. Example nighttime reverse scan signal levels—band 1.

exhibited both patterns, but one was dominant). One pattern was exemplified by band 1 detector 4 with a peak-to-peak amplitude of 2.0 DN, the other by band 7 detector 7. These two patterns were labeled 'form #1' and 'form #2', respectively (later labeled 'type 4-1' and 'type 4-7', respectively, by Barker (1984)).

## METHODS

All analyses to characterize the radiometry of the sensors were performed on digital computer compatible tape (CCT) data. Several types of CCT data were used, representing various stages of ground processing as well as calibration data. The analyses described in this paper generally were performed on full-frame TM image data, both to characterize full-frame effects and to take advantage of the large data volume (approximately 37 million pixels per band per frame) to improve the quality of the statistics generated.

Two primary methods were used to average the full-frame image data. In one case, to examine scan-angle effects, average scan lines were computed by averaging the columns of pixels down the entire frame. To analyze scan-direction effects, these average scan lines were stratified by scan direction, with the forward and reverse scan data being treated separately. The other type of averaging involved computing down-track profiles by averaging the rows of pixels across the entire frame, thereby computing an average signal value for each scan line. Each of these analyses was performed separately for each band and each detector of the sensors.

Earlier investigations by the authors (Malila *et al.*, 1984) demonstrated the value of using reflective-band (bands 1–5 and 7) TM data collected at

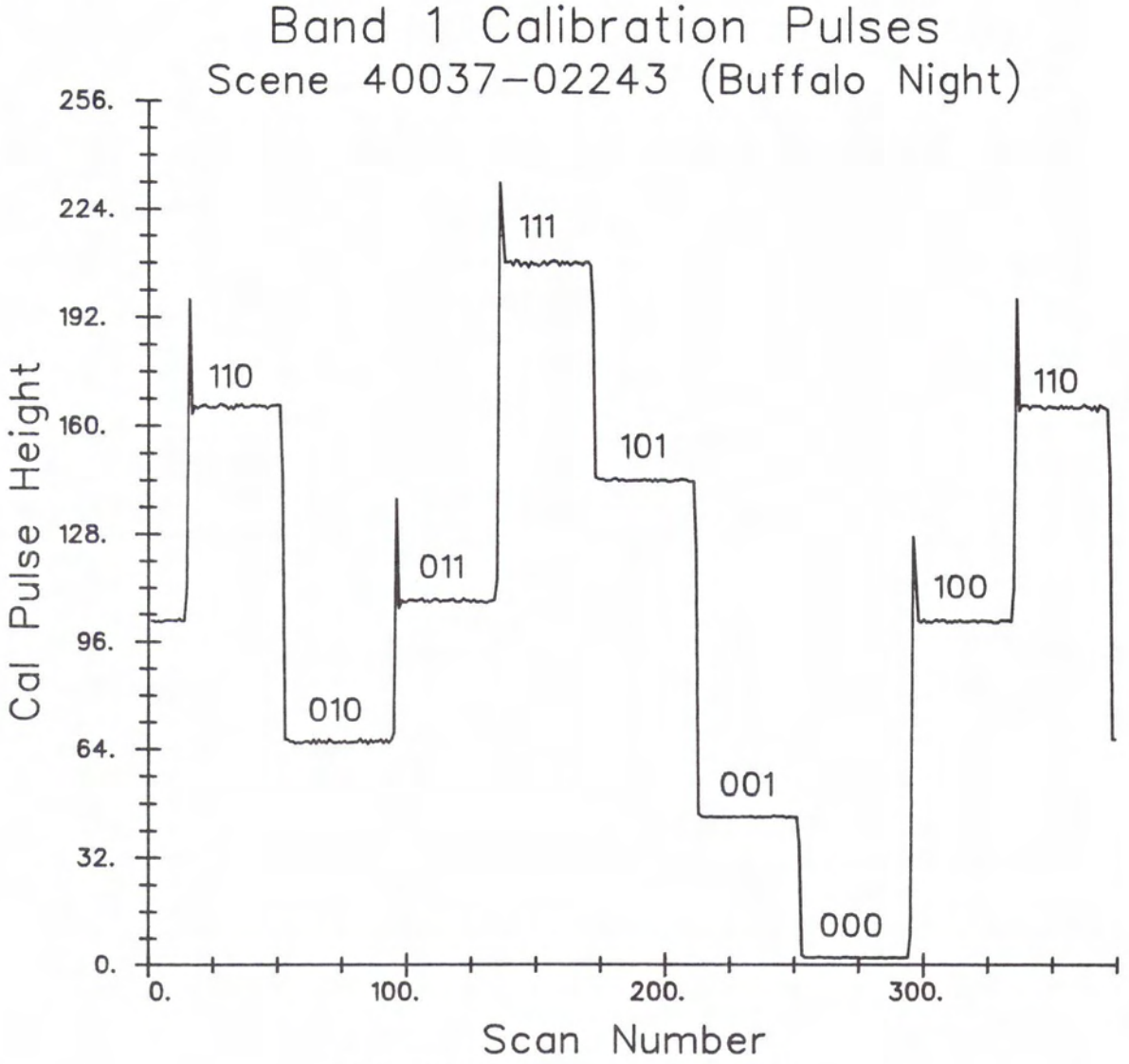


FIG. 3. Calibration lamp sequencing for band 1.

night for analysis of sensor data anomalies. The sensor sensitivities are such that no scene radiance is recorded, so any variations in the data are due to sensor noise effects. We again made extensive use of nighttime data in the analyses described herein, processing the data using the techniques described above.

Two techniques were employed to compare the radiometry of the Thematic Mappers on Landsat-4 and on Landsat-5, using a special data set which was collected simultaneously with both sensors. The first technique involved selecting a subimage of 3,564,000 pixels (1980 lines by 1800 pixels) from the Landsat-5 image and spatially registering it to the Landsat-4 TM image data. This registration was performed to subpixel accuracy using 50 control points and nearest neighbor resampling. The data in each subimage were averaged using $5 \times 5$ pixel cells to reduce any misregistration effects and to reduce the data volume while still retaining the data diversity. Linear regressions were performed with data from the two averaged images. Multiplicative and additive factors were computed for each band which can be used to relate the signals from one sensor to those expected from the other sensor for the same input radiance.

For the second comparison, histograms were computed for the subimages described above, and

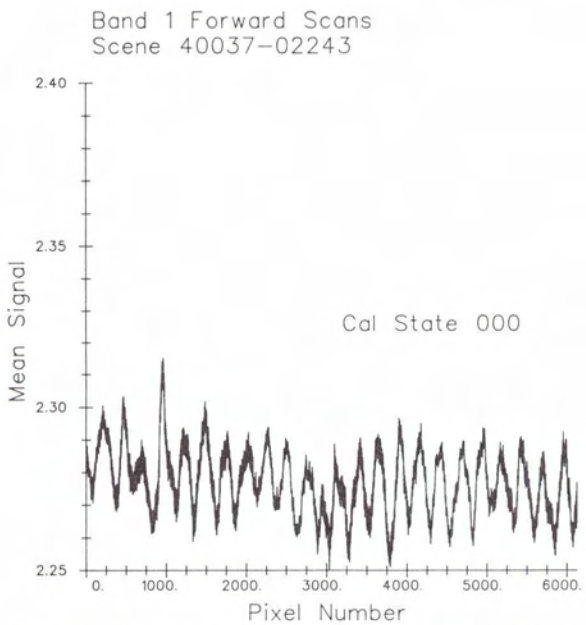


FIG. 4a. Nighttime forward scan signal rise for scans preceeded by calibration lamp state 000.

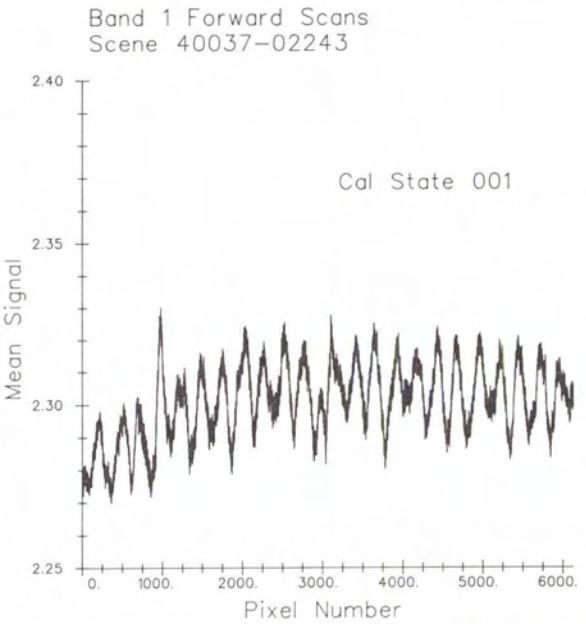


FIG. 4b. Nighttime forward scan signal rise for scans preceeded by calibration lamp state 001.

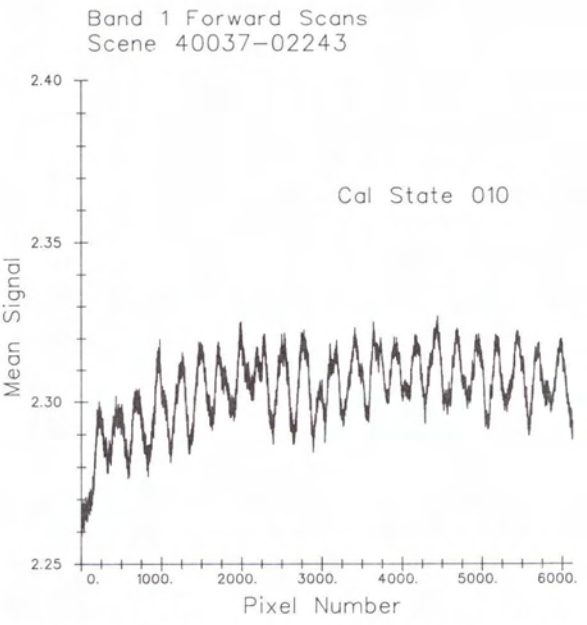


FIG. 4c. Nighttime forward scan signal rise for scans preceeded by calibration lamp state 010.

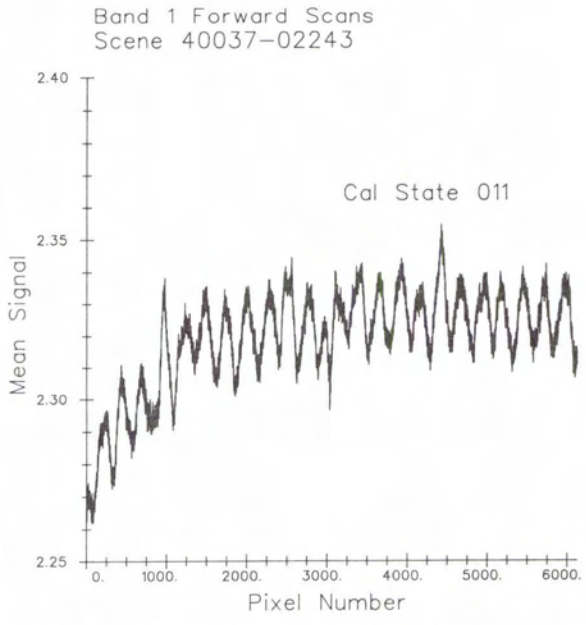


FIG. 4d. Nighttime forward scan signal rise for scans preceeded by calibration lamp state 011.

a histogram matching technique was employed to compute multiplicative and additive coefficients for relating data from one sensor to that of the other. Unlike the histogram matching procedure used in TM ground processing which equalizes means and standard deviations (Barker *et al.*, 1983), a procedure based on matching the cumulative distribution functions of the two data sets was employed. This technique is believed to have some advantages in making better use of the full range and distribution

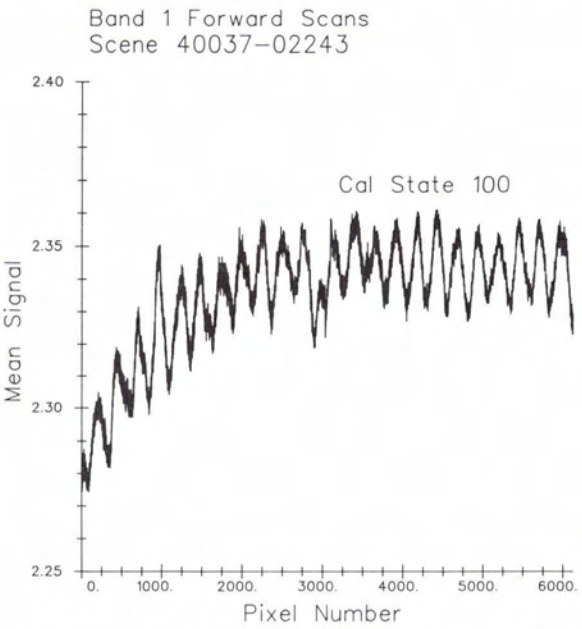


FIG. 4e. Nighttime forward scan signal rise for scans preceeded by calibration lamp state 100.

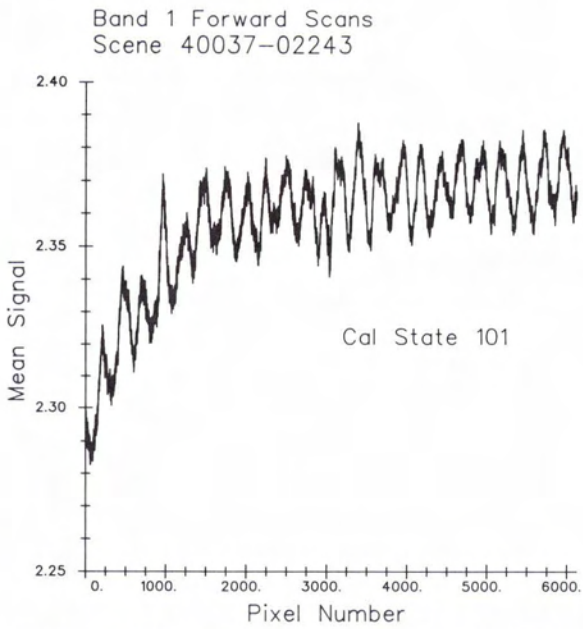


FIG. 4f. Nighttime forward scan signal rise for scans preceeded by calibration lamp state 101.

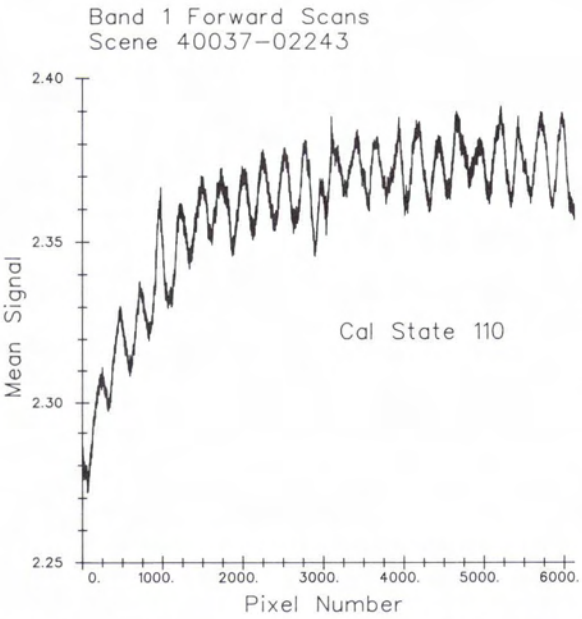


FIG. 4g. Nighttime forward scan signal rise for scans preceeded by calibration lamp state 110.

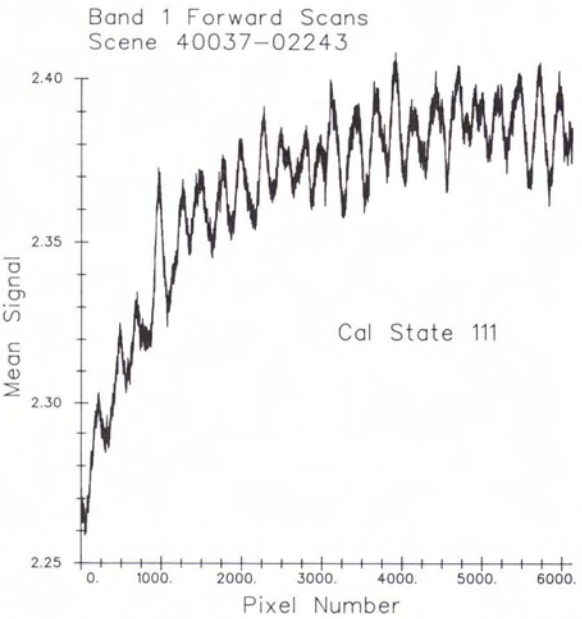


FIG. 4h. Nighttime forward scan signal rise for scans preceeded by calibration lamp state 111.

of data values in the histogram. Additionally, the histogram matching approach has much less stringent registration requirements than pixel or region matching approaches. For a region with a very small perimeter/area ratio, effects of slight misregistration would be minimal. The cumulative distribution function gives percentage of observations having signal values less than or equal to the designated

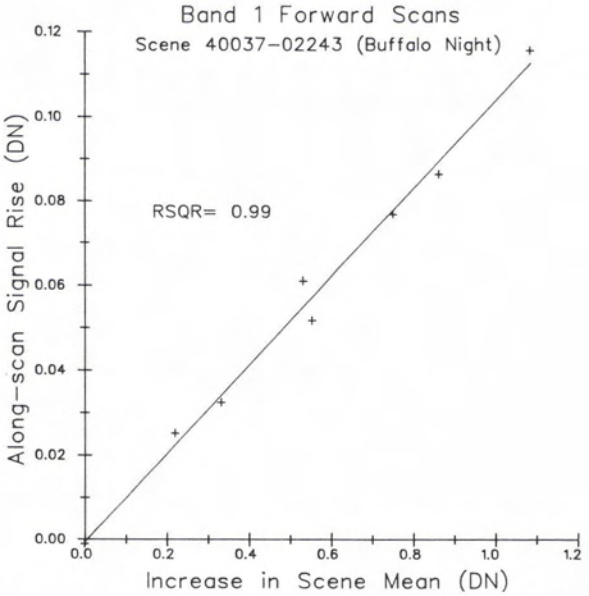


FIG. 5. Relationship of magnitude of signal rise and difference between scan-cycle mean and scene mean.

signal value. Interpolations were made to obtain the signal values corresponding to integer percentage values. Excluding end points, a regression of the corresponding percentile signal levels from the two sensors provided the desired correction coefficients.

## RESULTS

### Within-Line Droop

The single nighttime Landsat-5 TM scene (ID 5-0052-02182, Harrisburg, PA) available to us was used to quantify the within-scan droop/rise effect in Landsat-5 TM data. The average nighttime scan lines for band 4 of Landsat-5 TM are illustrated in Figure 1, along with data from Landsat-4 TM for comparison. Both forward and reverse scans are shown. The *y*-axes all have the same scale, i.e., 0.1 DN full scale, to facilitate comparison between sensors. Note that for reverse scans, pixel position 6000 is sampled prior to pixel position 1. Therefore, the effect is seen to be a signal rise with increasing time for both forward and reverse scans. In general, the within-scan rise has the same magnitude and time constant for the same band in each sensor. Magnitudes are greater in daytime data and the signals droop with increasing time, as will be discussed later.

Band 1 displays the greatest effect, with the mean reverse-scan signal increasing approximately 0.1 DN during the active scan. A simplified exponential decay model was fitted to the data for each of bands 1 through 4. For these bands, the time constant (time for magnitude of effect to decay to 1/e of original value) which produced the best fit ranged from 900 to 1100 pixel sample times, (approximately 9–10 milliseconds) for both Landsat-4 and Landsat-5 TM.

The mathematical model used is expressed by the equation:

$$S(p) = S_0 + Be^{-p/T} \quad (1)$$

Where:

$S(p)$ = signal returned by sensor for pixel $p$
$S_0$ = signal for $p$ equal to infinity
$B$ = magnitude of total droop/rise
$T$ = time (pixels) required for signal to change by 63% of $B$
$p$ = pixel number, with count starting with first image pixel (west-most for forward scans, east-most for reverse daytime scans).

Since the magnitude and time constant of the nighttime within-scan rise are essentially identical for Landsat-4 and Landsat-5, we would expect the daytime droop effects to be similar also. During daytime data acquisition when signal levels were much higher, we observed in Landsat-4 TM data a corresponding increase in the magnitude of the droop effect. In a daytime band 1 scene (ID 4-0049-16262) which had a scene mean of 61.9 DN, the magnitude of the droop was observed to be approximately minus 1.5 DN, with a time constant equivalent to approximately 900 pixels. At night, the magnitude of the rise was <0.15 DN, still with a time constant of 900 pixels for band 1. The mean scene level at night was 2.3 DN. Although qualitatively the daytime Landsat-5 effect appears similar to the daytime Landsat-4 effect, quantification of this effect in daytime Landsat-5 TM data awaits analysis of an appropriate scene in which variations in scene radiance have a relatively uniform spatial distribution.

The droop/rise effect was analyzed further to establish a hypothesis for its cause and a model for its description and potential use in correction. While the magnitude of the effect does not appear to be strictly proportional to the scene mean, it does appear as if the droop or rise is a drift toward the scan-cycle mean signal of the scene which also includes the signal values produced during shutter obscuration, calibration pulse, and DC restoration. This scan-cycle mean would be lower than the scene mean during the daytime due to the addition of the data acquired during shutter obscuration, and would be greater than the scene mean during nighttime data acquisition, where the scene itself is effectively a continuation of the shutter obscuration, and the calibration pulses drive the scan-cycle mean to a level slightly higher than the scene mean (see Figure 2). The hypothesis is that a-c coupling exists between the detector output and the analog-to-dig-

TABLE 1. MAGNITUDE AND PHASE OF LEVEL-SHIFT NOISE IN LANDSAT-4 SCENE 4-0161-02481

| | | Amplitude* | | Separation of States (#S.D.) | | | | Amplitude* | | Separation of States (#S.D.) | |
|---|---|---|---|---|---|---|---|---|---|---|---|
| Band | Det | Form 1 | Form 2 | Form 1 | Form 2 | Band | Det | Form 1 | Form 2 | Form 1 | Form 2 |
| 1 | 1 | 0.261 | −0.162 | 3.1 | 1.9 | 4 | 1 | 0.256 | −0.047 | 6.6 | 1.2 |
| 1 | 2 | −0.024 | −0.188 | .3 | 2.5 | 4 | 2 | 0.147 | −0.084 | 3.3 | 1.9 |
| 1 | 3 | 0.077 | −0.117 | 1.1 | 1.7 | 4 | 3 | 0.197 | −0.031 | 2.3 | .4 |
| 1 | 4 | 1.880 | 0.116 | 26.2 | 1.6 | 4 | 4 | 0.052 | −0.072 | 1.3 | 1.8 |
| 1 | 5 | 0.120 | −0.141 | 2.1 | 2.4 | 4 | 5 | 0.119 | −0.013 | 3.7 | .4 |
| 1 | 6 | 0.038 | −0.060 | .5 | .8 | 4 | 6 | 0.316 | −0.063 | 5.2 | 1.0 |
| 1 | 7 | 0.098 | −0.077 | 1.6 | 1.2 | 4 | 7 | 0.073 | −0.017 | 3.1 | .7 |
| 1 | 8 | 0.569 | −0.092 | 8.0 | 1.3 | 4 | 8 | 0.003 | −0.083 | .1 | 2.4 |
| 1 | 9 | 0.146 | 0.043 | 2.0 | .6 | 4 | 9 | 0.064 | −0.023 | 1.9 | .7 |
| 1 | 10 | 0.877 | −0.053 | 13.2 | .8 | 4 | 10 | 0.147 | −0.013 | 5.0 | .4 |
| 1 | 11 | 0.173 | −0.063 | 2.1 | .8 | 4 | 11 | 0.101 | −0.017 | 4.0 | .6 |
| 1 | 12 | 1.601 | −0.011 | 24.3 | .2 | 4 | 12 | 0.252 | 0.019 | 7.0 | .5 |
| 1 | 13 | 0.313 | −0.029 | 3.8 | .3 | 4 | 13 | 0.063 | −0.008 | 4.5 | .6 |
| 1 | 14 | 0.084 | −0.124 | 1.2 | 1.8 | 4 | 14 | 0.087 | −0.020 | 3.2 | .7 |
| 1 | 15 | 0.171 | −0.041 | 1.8 | .4 | 4 | 15 | 0.114 | −0.015 | 5.2 | .6 |
| 1 | 16 | −0.025 | −0.123 | .3 | 1.6 | 4 | 16 | 0.371 | 0.029 | 9.7 | .7 |
| 2 | 1 | 0.246 | −0.323 | 4.0 | 5.2 | 5 | 1 | −0.018 | 0.060 | .6 | 2.2 |
| 2 | 2 | 0.149 | 0.056 | 3.0 | 1.1 | 5 | 2 | 0.136 | −0.105 | 3.6 | 2.8 |
| 2 | 3 | −0.082 | −0.202 | 1.2 | 3.0 | 5 | 3 | −0.125 | −0.067 | 4.6 | 2.5 |
| 2 | 4 | 0.203 | 0.027 | 5.0 | .7 | 5 | 4 | 0.113 | −0.038 | 3.3 | 1.1 |
| 2 | 5 | 0.072 | −0.138 | 1.4 | 2.7 | 5 | 5 | −0.183 | −0.043 | 6.6 | 1.5 |
| 2 | 6 | 0.075 | 0.056 | 1.4 | 1.1 | 5 | 6 | 0.046 | −0.085 | 1.4 | 2.6 |
| 2 | 7 | 0.004 | −0.086 | .1 | 2.0 | 5 | 7 | 0.017 | 0.143 | .5 | 4.8 |
| 2 | 8 | 0.106 | 0.062 | 1.8 | 1.1 | 5 | 8 | −0.074 | −0.200 | 2.6 | 6.9 |
| 2 | 9 | 0.039 | −0.053 | 1.3 | 1.8 | 5 | 9 | −0.085 | 0.023 | 2.7 | .7 |
| 2 | 10 | 0.033 | 0.031 | 1.3 | 1.2 | 5 | 10 | −0.086 | 0.744 | 2.7 | 22.7 |
| 2 | 11 | 0.056 | −0.061 | 1.4 | 1.5 | 5 | 11 | −0.022 | 0.046 | .9 | 1.9 |
| 2 | 12 | 0.143 | 0.035 | 3.7 | .9 | 5 | 12 | 0.006 | 0.061 | .3 | 2.6 |
| 2 | 13 | 0.084 | −0.101 | 1.7 | 2.1 | 5 | 13 | −0.083 | 0.004 | 3.4 | .2 |
| 2 | 14 | 0.064 | 0.043 | 1.7 | 1.2 | 5 | 14 | −0.079 | −0.082 | 3.8 | 3.9 |
| 2 | 15 | 0.097 | −0.099 | 2.5 | 2.6 | 5 | 15 | −0.211 | −0.119 | 8.3 | 4.6 |
| 2 | 16 | 0.074 | 0.127 | 1.8 | 3.1 | 5 | 16 | −0.017 | −0.100 | .7 | 4.3 |
| 3 | 1 | 0.484 | −0.494 | 7.3 | 7.5 | 7 | 1 | −0.034 | 0.302 | 1.3 | 11.5 |
| 3 | 2 | 0.296 | 0.273 | 7.3 | 6.7 | 7 | 2 | 0.054 | −0.293 | 1.8 | 9.7 |
| 3 | 3 | 0.235 | −0.275 | 4.9 | 5.3 | 7 | 3 | −0.090 | 0.342 | 3.1 | 11.8 |
| 3 | 4 | 0.022 | 0.032 | .7 | .9 | 7 | 4 | 0.093 | −0.273 | 3.4 | 9.9 |
| 3 | 5 | 0.304 | −0.205 | 6.0 | 4.0 | 7 | 5 | −0.006 | 0.281 | .2 | 10.8 |
| 3 | 6 | 0.248 | 0.086 | 5.7 | 2.0 | 7 | 6 | 0.123 | −0.308 | 4.3 | 10.4 |
| 3 | 7 | 0.155 | −0.203 | 3.6 | 4.8 | 7 | 7 | −0.040 | 0.960 | .3 | 6.4 |
| 3 | 8 | −0.088 | −0.034 | 2.1 | .8 | 7 | 8 | 0.066 | −0.345 | 2.6 | 13.5 |
| 3 | 9 | −0.051 | −0.063 | 1.2 | 1.4 | 7 | 9 | −0.109 | 0.197 | 4.2 | 7.5 |
| 3 | 10 | 0.253 | 0.055 | 4.0 | .9 | 7 | 10 | 0.095 | −0.461 | 3.3 | 15.1 |
| 3 | 11 | 0.003 | −0.134 | .2 | 4.0 | 7 | 11 | −0.045 | 0.232 | 1.6 | 8.5 |
| 3 | 12 | 0.102 | 0.230 | 1.9 | 4.2 | 7 | 12 | 0.168 | −0.297 | 5.3 | 9.1 |
| 3 | 13 | 0.215 | −0.151 | 5.6 | 3.9 | 7 | 13 | −0.087 | 0.224 | 2.8 | 7.1 |
| 3 | 14 | 0.209 | 0.180 | 4.2 | 3.6 | 7 | 14 | 0.198 | −0.085 | 6.6 | 2.8 |
| 3 | 15 | 0.278 | −0.262 | 6.9 | 6.5 | 7 | 15 | −0.043 | 0.193 | 1.7 | 7.7 |
| 3 | 16 | 0.446 | 0.782 | 6.9 | 12.1 | 7 | 16 | 0.169 | −0.253 | 5.5 | 8.2 |

* Negative amplitudes indicate level shifts with phase shifts of 180° relative to B1D4 (Form 1) or B7D7 (Form 2).

ital converter, producing a signal decay proportional to the departure from the scan-cycle mean.

To test this hypothesis, a scene of nighttime Landsat-4 TM data (scene 4-0037-02243) was segmented based on the calibration lamp state observed by the sensors prior to each scan. As illustrated in Figure 3, the internal calibration lamps sequence through the eight possible states, re-

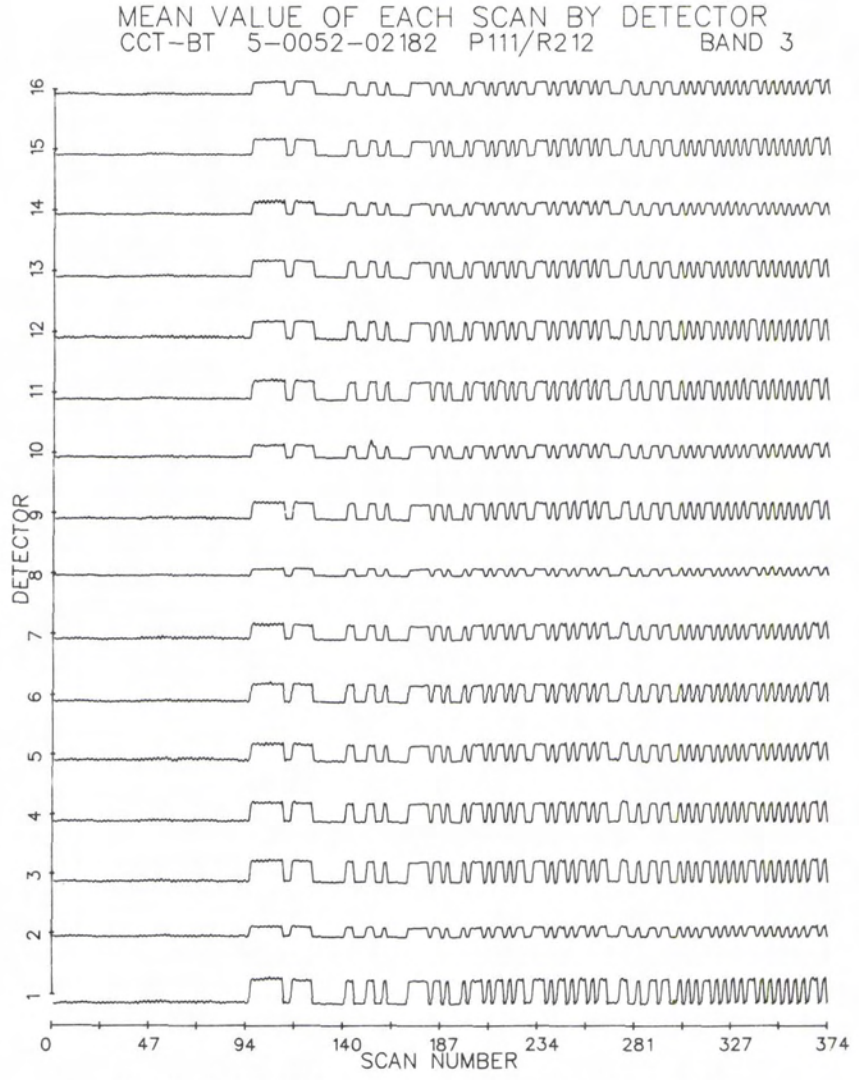


FIG. 6. Level shifts for Landsat-5 TM band 3 nighttime data.

maining in each state for approximately 40 scans (20 forward/reverse scan cycles). During nighttime reflective-band data collection, the signal pulses resulting from viewing these calibration lamps at the end of each scan are the only signals available to shift the scan-cycle mean from the scene mean. All scans with lamp state 000 (no lamps on) were grouped into one subimage, and seven other subimages were created for the other seven lamp states (001, 010, 011, 100, 101, 110, and 111, where each binary digit represents the state of one of the three calibration lamps). Average scan-lines were computed for each of these subimages, then smoothed and displayed as plots of mean signal level versus pixel position (see Figures 4a–4h). Qualitatively one can see that the effect is greatest when the calibration pulse adds the most to the scan-cycle mean (state 111, all lamps on), and is nonexistent in the case of no calibration pulse (scan-cycle mean equal to scene mean).

Quantitative support for the hypothesis of drift toward a scan-cycle mean was derived from data on the calibration tape (CCT-ADDS) associated with the image data. From the CCT-ADDS, the magnitude of the calibration pulse for each scan line could be computed, which in turn allowed calculation of the scan-cycle mean for each scan. The rise for each scan was computed and plotted against the difference between scan-cycle mean and scene mean as illustrated in Figure 5. Regression analysis indicated

TABLE 2. MAGNITUDE AND PHASE OF LEVEL-SHIFT NOISE IN LANDSAT-5 SCENE 5-0052-02182

| Band | Det | Amplitude* | Separation of States (Number of Std. Dev.) | Band | Det | Amplitude* | Separation of States (Number of Std. Dev.) |
|---|---|---|---|---|---|---|---|
| 1 | 1 | 0.036 | 0.9 | 4 | 1 | 0.285 | 11.0 |
| 1 | 2 | −0.229 | 6.4 | 4 | 2 | 0.150 | 5.5 |
| 1 | 3 | 0.061 | 1.7 | 4 | 3 | 0.149 | 5.0 |
| 1 | 4 | −0.184 | 4.2 | 4 | 4 | 0.205 | 8.4 |
| 1 | 5 | 0.044 | 1.3 | 4 | 5 | 0.044 | 3.3 |
| 1 | 6 | −0.249 | 6.3 | 4 | 6 | 0.045 | 2.5 |
| 1 | 7 | 0.113 | 3.4 | 4 | 7 | 0.025 | 3.1 |
| 1 | 8 | −0.208 | 5.2 | 4 | 8 | 0.016 | 0.6 |
| 1 | 9 | 0.042 | 1.3 | 4 | 9 | 0.078 | 2.8 |
| 1 | 10 | −0.303 | 9.3 | 4 | 10 | 0.004 | 0.3 |
| 1 | 11 | 0.068 | 2.3 | 4 | 11 | 0.106 | 3.8 |
| 1 | 12 | −0.216 | 5.4 | 4 | 12 | 0.016 | 0.7 |
| 1 | 13 | −0.010 | 0.3 | 4 | 13 | 0.138 | 4.4 |
| 1 | 14 | −0.307 | 8.5 | 4 | 14 | 0.081 | 2.2 |
| 1 | 15 | 0.001 | 0.0 | 4 | 15 | 0.085 | 3.0 |
| 1 | 16 | −0.266 | 7.6 | 4 | 16 | 0.015 | 0.5 |
| 2 | 1 | 0.523 | 16.3 | 5 | 1 | 0.135 | 6.8 |
| 2 | 2 | 0.084 | 4.6 | 5 | 2 | 0.006 | 0.4 |
| 2 | 3 | 0.239 | 11.5 | 5 | 3 | 0.190 | 13.6 |
| 2 | 4 | −0.009 | 1.1 | 5 | 4 | −0.023 | 1.7 |
| 2 | 5 | 0.178 | 10.5 | 5 | 5 | −0.067 | 4.5 |
| 2 | 6 | 0.070 | 7.2 | 5 | 6 | −0.128 | 9.3 |
| 2 | 7 | 0.157 | 8.7 | 5 | 7 | 0.008 | 0.6 |
| 2 | 8 | 0.065 | 7.3 | 5 | 8 | −0.115 | 9.0 |
| 2 | 9 | 0.079 | 8.2 | 5 | 9 | 0.056 | 4.3 |
| 2 | 10 | 0.012 | 2.4 | 5 | 10 | 0.019 | 0.5 |
| 2 | 11 | 0.086 | 6.9 | 5 | 11 | 0.100 | 7.4 |
| 2 | 12 | 0.016 | 2.3 | 5 | 12 | −0.129 | 6.9 |
| 2 | 13 | 0.177 | 9.5 | 5 | 13 | 0.022 | 1.7 |
| 2 | 14 | 0.075 | 8.4 | 5 | 14 | −0.074 | 5.0 |
| 2 | 15 | 0.159 | 10.1 | 5 | 15 | −0.088 | 7.4 |
| 2 | 16 | 0.263 | 12.6 | 5 | 16 | −0.137 | 9.7 |
| 3 | 1 | 0.470 | 14.1 | 7 | 1 | 0.019 | 1.1 |
| 3 | 2 | 0.196 | 8.1 | 7 | 2 | −0.013 | 0.8 |
| 3 | 3 | 0.437 | 14.3 | 7 | 3 | −0.050 | 3.1 |
| 3 | 4 | 0.389 | 13.9 | 7 | 4 | −0.110 | 6.8 |
| 3 | 5 | 0.317 | 8.2 | 7 | 5 | 0.001 | 0.1 |
| 3 | 6 | 0.340 | 12.0 | 7 | 6 | −0.095 | 6.6 |
| 3 | 7 | 0.286 | 7.8 | 7 | 7 | 0.146 | 8.9 |
| 3 | 8 | 0.141 | 8.5 | 7 | 8 | −0.159 | 10.2 |
| 3 | 9 | 0.326 | 10.5 | 7 | 9 | 0.161 | 11.7 |
| 3 | 10 | 0.250 | 9.4 | 7 | 10 | −0.156 | 9.4 |
| 3 | 11 | 0.371 | 12.9 | 7 | 11 | 0.107 | 7.0 |
| 3 | 12 | 0.351 | 11.8 | 7 | 12 | −0.060 | 4.1 |
| 3 | 13 | 0.318 | 12.8 | 7 | 13 | 0.032 | 2.3 |
| 3 | 14 | 0.237 | 7.7 | 7 | 14 | −0.038 | 2.1 |
| 3 | 15 | 0.321 | 12.6 | 7 | 15 | 0.022 | 1.6 |
| 3 | 16 | 0.257 | 11.8 | 7 | 16 | −0.116 | 8.0 |

* Negative amplitudes indicate level shifts with phase shifts of 180° relative to band 3 detectors.

an excellent fit ($R^2$ of 0.99), which strongly supports the hypothesis, indicating that the parameter $B$ in the model expressed above is a function of the difference between the scan-cycle mean and the scene mean. Although this analysis was performed only for forward scans of band 1 of one Landsat-4 TM image, experience to date indicates that the result may be extended to both scan directions of bands 1 through 4 of both Landsat-4 and Landsat-5 Thematic Mappers with a high degree of confidence.

This droop/rise effect has been observed for the primary focal plane bands only. For both Landsats, bands 5 and 7 show essentially no change in mean signal level within the scan line, with perhaps a

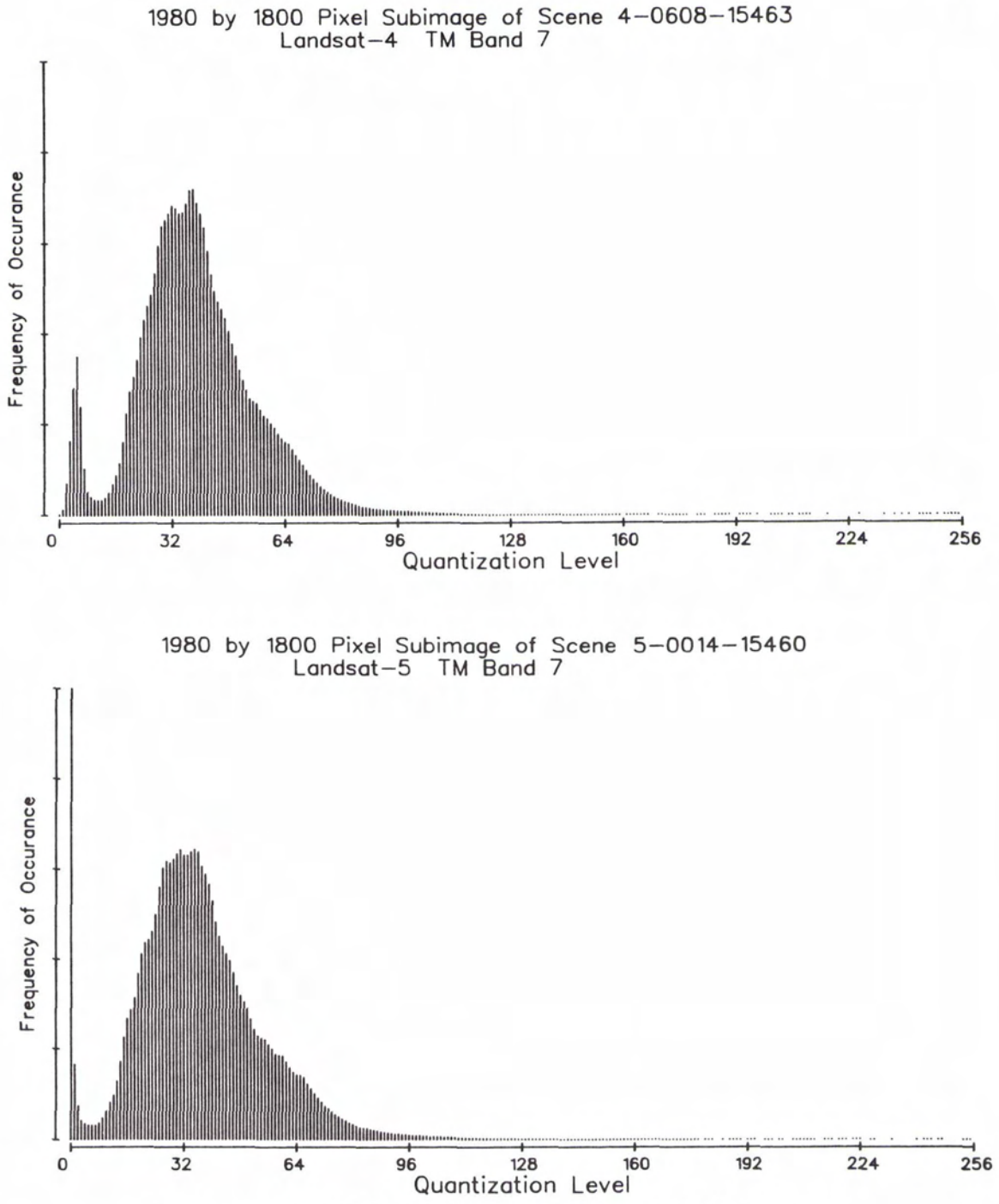


FIG. 7. Landsat-4 and Landsat-5 TM band 7 histograms for coincident regions.

slight change in the *opposite* direction to that seen in bands 1 through 4. Band 6 mean signal levels have been observed to change within scan lines in a variety of patterns. Detailed analysis of potential within-scan effects in band 6 is made more difficult by the absence of any constant scene data comparable to the nighttime data in the reflective bands. Even a completely uniform ground scene would

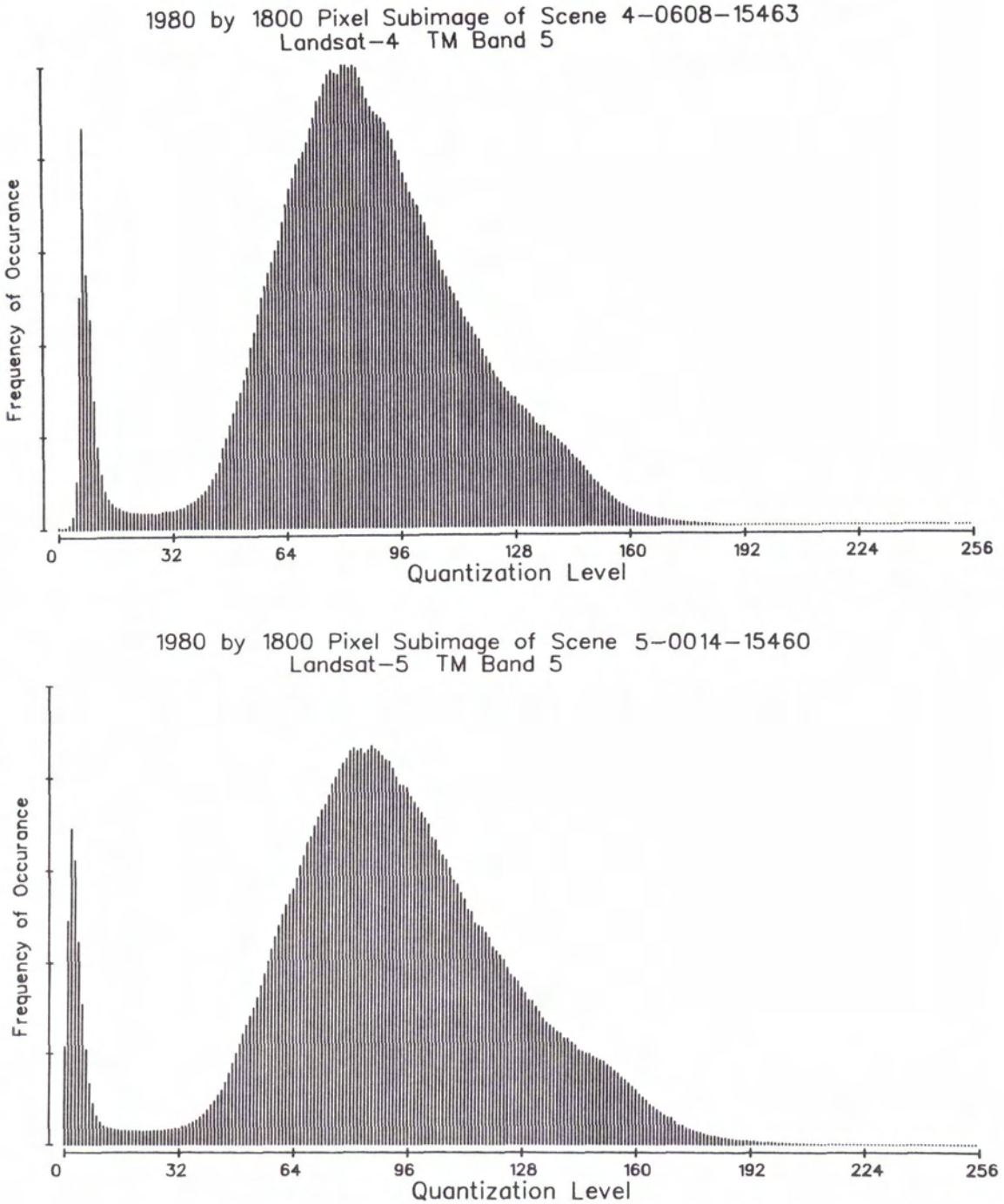


FIG. 8. Landsat-4 and Landsat-5 TM band 5 histograms for coincident regions.

have varying atmospheric effects in different parts of the scene.

This droop effect should not cause serious problems for most users. However, it can confound attempts to extend signatures from one side of a scene to the other and can introduce banding (stripes 16 lines wide, or 17 lines in geometrically corrected CCT-PT data) at the scene edges. Implementation of the proposed exponential model would require pixel-by-pixel correction and could prove costly in

terms of computation time. It is our understanding that NASA and NOAA will leave it to the individual users to determine the importance of correcting for this effect and actually performing the correction.

Also apparent in Figures 4a–4h are oscillations superimposed on the rise effect. These oscillations are coherent noise found in all reflective bands of both Landsat-4 and Landsat-5. Although quite obvious in these plots derived from nighttime data, the peak-to-peak amplitudes are quite small (<0.75 DN in unfiltered data, <0.05 DN in these smoothed plots) and have not been observed in daytime data. The cause of this approximately 400 Hz (262–264 pixel period) noise is undetermined.

### Scan-Correlated Level Shifts

In the Landsat-4 TM data we have examined, type 4-7 scan-correlated level shifts are always present, and the signals often shift states with a regular period. Scan-correlated shifts of type 4-1 are present in most, but not all data, and the type 4-1 pattern tends to remain in one state or the other for several scans of the scan mirror. The peak-to-peak amplitude for each affected detector for each form of the shift is essentially constant in all cases where that form of the noise exists. The phase relationships between the affected detectors also remain constant in all images (i.e., band 7 detector 7 is always in its high type 4-7 state when band 5 detector 8 is in its low type 4-7 state). Figure 14 of Malila *et al.* (1984) illustrated both patterns of level shift for the 16 band 1 detectors of Landsat-4 TM for a night scene. Relative magnitudes and phases are readily apparent from the illustrations. Table 1 provides the quantitative results, giving the magnitude and phase of each level-shift pattern for the 96 Landsat-4 TM reflective-band detectors.

Initial analyses of Landsat-5 TM data indicated a similar effect, but with only one pattern (Malila and Metzler, 1984; Barker 1984). We examined nighttime reflective-band data to provide quantification of the magnitude and phase relationships of the effect. Figure 6 illustrates the level shifts for band 3 of Landsat-5 TM, the band most affected by this noise. The plots were produced by computing the mean signal level for each scan for each detector of each band and by plotting these scan-line means versus the scan number. In these plots, the maximum peak-to-peak amplitude is approximately 0.5 DN. Table 2 contains the quantitative results for the reflective-band detectors of the Landsat-5 TM. It can be seen that nearly all detectors are affected, although the magnitude is very low (<0.1 DN) for many. Band 3 shows the greatest effect although band 2 detector 1 is the single most affected detector with a level shift >0.5 DN. The compares with the maximum shift of 2.0 DN measured for Landsat-4 band 1 detector 4. Several detectors did not display any measurable effect in this scene. They are: band 1 detectors 1, 3, 5, 9, 13, and 15; band 2 detector 4; band 4 detectors 8, 10, 12, and 16; band 5 detectors 2, 4, 7, 10, and 13; and band 7 detectors 1, 2, 5, and 15. As seen in Landsat-4 TM data, patterns of phase and magnitude of the level-shift effect within a band often place the detectors into odd-even groups. As with the within-scan droop, the confounding effect of scene data prevents analysis of this type for band 6. For this band, shutter data may be used to quantify any level shifts but with somewhat lowered precision.

Although these level-shifts are strikingly evident in the nighttime reflective data, where the scene makes no contribution to the observed signal level, they are of the same magnitude in daytime data and even there can cause noticeable striping. The magnitude of these shifts and the large number of scenes in which they occur places a high value on the correction of the effect for some applications. Fortunately, the constancy of the magnitude permits relatively simple correction techniques. Since the level shift remains constant for the entire scan, the shifts are also observable in the shutter data collected at the ends of each scan line. Based on this, several methods of correcting for level shifts have been proposed which appear effective in reducing the effect

TABLE 3. COEFFICIENTS FOR CONVERTING LANDSAT-4 DN TO LANDSAT-5 DN (SCENES 4-0608-15463 and 5-0014-15460, 15 MARCH 1984)

Landsat-5 TM = $A$*(Landsat-4 TM) + $B$

| Band | $A$ | $B$ | S.E. | $R^2$ | Range of Data Values (DN) Landsat-4 | Landsat-5 |
|---|---|---|---|---|---|---|
| 1 | 1.0438 | −3.538 | 0.151 | 0.99943 | 73-109 | 73-111 |
| 2 | 1.1200 | −2.719 | 0.134 | 0.99922 | 26-52 | 26-56 |
| 3 | 0.9869 | −3.678 | 0.142 | 0.99975 | 26-77 | 22-72 |
| 4 | 1.0030 | −4.627 | 0.078 | 0.99995 | 11-92 | 7-88 |
| 5 | 1.1452 | −7.330 | 0.106 | 0.99999 | 6-154 | 0-169 |
| 6 | 1.0040 | −0.711 | 0.119 | 0.99956 | 114-148 | 113-148 |
| 7 | 1.0923 | −6.244 | 0.054 | 0.99999 | 3-86 | 0-88 |

Note: If the DN computed for Landsat-5 is <0, substitute 0. If it is >255, substitute 255.

TABLE 4. COEFFICIENTS FOR CONVERTING LANDSAT-5 DN TO LANDSAT-4 DN (SCENES 4-0608-15463 AND 5-0014-15460, 15 MARCH 1984)

| Landsat-4 TM = A*(Landsat-5 TM) + B | | | | | | |
|---|---|---|---|---|---|---|
| | | | | | Range of Data Values (DN) | |
| Band | A | B | S.E. | $R^2$ | Landsat-4 | Landsat-5 |
| 1 | 0.9580 | 3.390 | 0.145 | 0.99943 | 73-109 | 73-111 |
| 2 | 0.8928 | 2.427 | 0.120 | 0.99922 | 26-52 | 26-56 |
| 3 | 1.0132 | 3.726 | 0.144 | 0.99975 | 26-77 | 22-72 |
| 4 | 0.9970 | 4.614 | 0.078 | 0.99995 | 11-92 | 7-88 |
| 5 | 0.8732 | 6.401 | 0.093 | 0.99999 | 6-154 | 0-169 |
| 6 | 0.9960 | 0.714 | 0.118 | 0.99956 | 114-148 | 113-148 |
| 7 | 0.9155 | 5.717 | 0.049 | 0.99999 | 3-86 | 0-88 |

Note: If the DN computed for Landsat-4 is >255, substitute 255.

(Barker, 1984; Fischel, 1984; Kogut *et al.*, 1983; Malila *et al.*, 1984; Metzler and Malila, 1983a; Murphy *et al.*, 1984). The general approach is to detect the presence of the shift (normally by looking at shutter data), then to subtract (or add) the known magnitude of the shift to each pixel in the affected scan line.

### TM LANDSAT-4 VERSUS LANDSAT-5 RADIOMETRIC COMPARISON

Radiometric matching of the Landsat-4 and Landsat-5 TM sensors was facilitated by the availability of a unique set of radiometrically corrected data collected simultaneously by the two sensors and registered to subpixel accuracy as described above. Same-band images from the two sensors were very similar in appearance, although examination on an image display system required different gain and offset factors to be applied to achieve identical brightness and contrast for each pair of images. Since both the Landsat-4 and Landsat-5 scenes were processed through TIPS (Thematic mapper Image Processing System), it was expected that radiometrically corrected products would have essentially identical corrected signal values for the same scene viewed at the same time. In addition to multiplicative and additive differences, clipping of the Landsat-5 data values was obvious in both bands 5 and 7 at the low radiance end of the dynamic range. The band 7 low-level clipping is apparent from a histogram of signal-level frequency for band 7 for both Landsat-4 and Landsat-5 (see Figure 7). The pixels with values zero to six in the Landsat-4 scene are all mapped to value zero in the Landsat-5 scene. Although the offset was nearly as large for band 5 (see Figure 8), fewer data values actually were clipped (0.3 percent of the scene versus 4.2 percent in band 7).

As noted earlier, band-by-band comparisons were carried out using two different techniques: (1) regression of signal values from the coincident pixels or regions, and (2) regression of signal values associated with specific histogram percentile classes. When clipping was not present, either technique produced essentially the same results. Where clipping was present, regression of matched areas led to smaller additive terms and larger multiplicative terms, a result deemed erroneous after inspecting the histograms. For this reason, coefficients from the histogram matching approach are presented here. Table 3 presents the multiplicative and additive coefficients to convert Landsat-4 TM signal levels to Landsat-5 TM equivalent values; and Table 4 contains the coefficients to convert Landsat-5 signals to Landsat-4 values. It should be noted that while this was a simultaneously collected data set, and therefore nearly ideal for this type of analysis, the correction coefficients presented are valid only if ground processing parameters are not changed. It should also be noted that data which have been clipped as in Landsat-5 bands 5 and 7 can not be retrieved—all the zeroes in Landsat-5 band 7 data will be converted to sixes in Landsat-4 band 7, whereas Landsat-4 band 7 would have recorded the same pixels with signal levels ranging from zero to six. In using these conversion equations, resultant DNs less than zero should be assigned the value zero; DNs greater than 255 should be assigned 255.

Converting the pixel values to radiance levels via

TABLE 5. LANDSAT-4 AND LANDSAT-5 TM RADIANCE CONVERSION PARAMETERS (SCENES 4-0608-15463 AND 5-0014-15460, 15 MARCH 1984)

| Radiance = A0 + A1*DN (mW/(cm² sr μm)) | | | | |
|---|---|---|---|---|
| | A0 (mW/(cm² sr μm)) | | A1 (mW/(cm² sr μm))/DN | |
| Band | Landsat-4 | Landsat-5 | Landsat-4 | Landsat-5 |
| 1 | −0.1500 | −0.1500 | 0.06024 | 0.06024 |
| 2 | −0.2802 | −0.2805 | 0.11750 | 0.11750 |
| 3 | −0.1203 | −0.1194 | 0.08061 | 0.08059 |
| 4 | −0.1504 | −0.1500 | 0.08145 | 0.08143 |
| 5 | −0.0372 | −0.0370 | 0.01081 | 0.01081 |
| 6 | 0.1252 | 0.1238 | 0.00569 | 0.00563 |
| 7 | −0.1500 | −0.1500 | 0.00570 | 0.00568 |

TABLE 6. LANDSATS-4 AND LANDSAT-5 TM REGRESSIONS OF RADIANCE VALUES (SCENES 4-0608-15463 AND 5-0014-15460, 15 MARCH 1984)

Landsat-5 TM = $A$*(Landsat-4 TM) + $B$

| Band | $A$ | $B$ | S.E. | $R^2$ | Range of Radiance Values (mW/(cm$^2$ sr $\mu$m)) Landsat-4 | Landsat-5 |
|---|---|---|---|---|---|---|
| 1 | 1.0435 | −0.205 | 0.009 | 0.99943 | 4.25–6.44 | 4.23–6.52 |
| 2 | 1.1196 | −0.285 | 0.016 | 0.99922 | 2.76–5.87 | 2.79–6.28 |
| 3 | 0.9865 | −0.297 | 0.011 | 0.99975 | 1.98–6.06 | 1.67–5.68 |
| 4 | 1.0027 | −0.376 | 0.006 | 0.99995 | 0.77–7.33 | 0.42–6.98 |
| 5 | 1.1452 | −0.074 | 0.001 | 0.99999 | −.03–1.63 | −.03–1.79 |
| 6 | 0.9932 | −0.002 | 0.001 | 0.99956 | 0.77–0.97 | 0.76–0.96 |
| 7 | 1.0885 | −0.002 | 0.001 | 0.99999 | −.13–0.34 | −.15–0.35 |

the coefficients provided in the Radiometric Calibration Ancillary Record of the Leader File associated with each band of image data (NASA, 1983) did not resolve the discrepancy observed between the two sensors. Table 5 lists the multiplicative and additive coefficients extracted from tape headers and used in the conversion. Table 6 is similar to Table 3 in that it defines conversion of Landsat-4 signals to Landsat-5 equivalent signals but in terms of radiance instead of signal counts. It is not known at this time why the radiometrically corrected data are not more closely matched.

An additional discrepancy was noted between the previously published band 6 temperature sensitivity range and the range implied by the coefficients listed in Table 5. Using these coefficients to convert the range 0.255 DN to radiance gives a radiance range of 0.125 to 1.575 mW/(cm$^2$ sr $\mu$m), representing an apparent temperature range of approximately 200 to 340°K, not the advertised 260°K to 320°K. This causes an increase in the temperature difference represented by a change of 1 DN. The specified 260°K to 320°K temperature range actually spans approximately 63–196 DN versus the specified 0.255 DN. For Landsat-5 TM, the radiance range is very slightly different (0.124 to 1.560 mW/(cm$^2$ sr $\mu$m)), still giving a range of apparent temperature of approximately 200°K to 340°K (or a DN range of approximately 63–193 for apparent temperatures of 260°K to 320°K). Users unaware of these differences may incorrectly derive temperatures from TM band 6 data.

## SUMMARY

Landsat-5 TM image data were found to be quite similar to Landsat-4 TM data, both in terms of high overall quality and in the presence of several anomalies. Detailed analysis revealed a systematic within-scan drift (or droop/rise) of the signal from the scene mean toward the overall scan-cycle mean in spectral bands 1 through 4. The magnitude of this drift ranged from minus 1.5 DN (daytime) to +0.15 DN (nighttime), depending on scene content. The drift was fitted with a simple exponential decay model and found to have a time constant equivalent to about one-sixth of a frame width.

Scan-correlated level shifts are present in both Landsat-4 and Landsat-5 TM data. The maximum effect observed in Landsat-5 data was approximately 0.5 DN peak-to-peak, compared with a maximum of 2.0 DN observed in Landsat-4 data. The level-shifts appear to be present in most if not all images, and effective correction procedures have been proposed.

Although data from both Thematic Mappers are produced in radiometrically corrected form, comparison of data acquired simultaneously by the two sensors revealed significant differences in their calibration. In the reflective bands, the multiplicative factors required to convert Landsat-4 TM data to Landsat-5 data ranged from 0.987 to 1.145, with corresponding additive terms of −2.7 DN to −6.2 DN, and displayed evidence of low-level clipping in Landsat-5 bands 5 and 7. The thermal bands (band 6) were more closely matched, but are calibrated to have a full-range temperature range of 200°K to 340°K instead of the advertised 260°K to 320°K.

## REFERENCES

Barker, J. L., 1984. Relative Radiometric Calibration of Landsat TM Reflective Bands: *LANDSAT-4 Science Investigations Summary*, v. I, July, pp. 140-180.

Barker, J. L., Abrams, R. B., Ball, D. L., and Leung, K. C., 1983. Radiometric Calibration and Processing Procedure for Reflective Bands on Landsat-4 Proto-flight Thematic Mapper: *Proceedings of Landsat-4 Science Characterization Early Results Symposium*, v. II, NASA Conference Publication 2355, p. 75.

Fischel, D., 1984. Validation of the Thematic Mapper Radiometric and Geometric Correction Algorithms: *IEEE Transactions on Geoscience and Remote Sensing*, v. GE-22, no. 3, pp. 237-242.

Kieffer, H., Cook, D. A., Eliason, E. M., and Eliason, P. T., 1985. Intraband Radiometric Performance of the Landsat Thematic Mappers: *Photogrammetric Engineering and Remote Sensing*, (this issue).

Kogut, J., Larduinat, E., and Fitzgerald, M., 1983. An Analysis of New Techniques for Radiometric Correc-

tion of LANDSAT-4 Thematic Mapper Images: Research and Data Systems, Inc., Lanham, MD.

Malila, W. A., Metzler, M. D., Rice, D. P., and Crist, E. P., 1984. Characterization of LANDSAT-4 MSS and TM Digital Image Data: *IEEE Transactions on Geoscience and Remote Sensing*, v. GE-22, no. 3, pp. 177-191.

Metzler, M. D., and Malila, W. A., 1983a. Radiometric Characterization of Thematic Mapper Full-frame Imagery: in *Proceedings SPSE/ASP Conference on Techniques for Extraction of Information from Remotely Sensed Images*, Rochester, NY.

———, 1983b. Scan-angle and Detector Effects in Thematic Mapper Radiometry: *Proceedings of Landsat-4 Science Characterization Early Results Symposium*, January 1983, v. II, NASA Conference Publication 2355 pp. 421-441.

Malila, W. A., and Metzler, M. D., 1984. *Eighth Quarterly Progress Report for Study of Spectral-Radiometric Characteristics of the Thematic Mapper for Land Use Applications:* Environmental Research Institute of Michigan, Report No. 164000-13-P, October.

Murphy, J. M., Butlin, T., Duff, P. E., and Fitzgerald, A. J., 1984. Revised Radiometric Calibration Technique for LANDSAT-4 Thematic Mapper Data: *IEEE Transactions on Geoscience and Remote Sensing*, v. GE-22, no. 3, pp. 243-251.

National Aeronautics and Space Administration, 1983. Interface Control Document between the NASA Goddard Space Flight Center (GSFC) and the Department of Interior EROS Data Center (EDC) for Landsat-D Thematic Mapper Computer Compatible Tape (CCT-AT, CCT-PT), Revision A: NASA, no. LSD-ICD-105, p. 60.

## FIG CONGRESS '86

The Canadian Institute of Surveying will be hosting the XVIII Congress of the International Federation of Surveyors from June 1-11, 1986 in Toronto, Canada.

The Congress Organizing Committee is planning ten exciting days designed to fulfill all expectations of this international meeting, all centered around a technical program with a theme "**Inner and Outer Space—Limitless Horizons for the Surveyors**".

The Sheraton Centre Hotel in downtown Toronto, which will house all delegates and meetings, has provided the largest exhibit display ever offered to a FIG Congress.

Technical tours and excursions have also been organized to allow delegates an opportunity to see Canada from coast to coast. There are also exciting programs and functions for accompanying persons to take part in.

For a Registration Form or for further information please contact:

FIG CONGRESS '86
P.O. Box 186, Station Q
Toronto, Ontario, Canada
M4T 1M2